AD-A106 386 UNIVERSITY COLL LONDON (ENGLAND) DEPT OF PHYSICS AND--ETC F/G 4/1
TROPOSPHERIC - STRATOSPHERIC TIDAL INVESTIGATIONS. PART III. HO--ETC(U)
AUG 81 G V GROVES, A WILSON AFOSR-77-3224

UNCLASSIFIED AFGL-TR-81-0301 NL

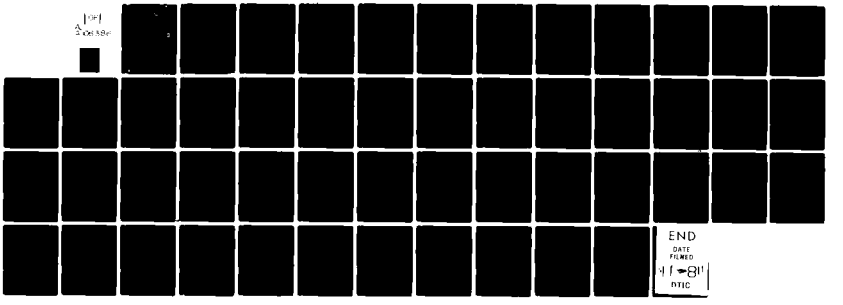

END
DATE FILMED
11-81
DTIC

Grant number: AFOSR – 77 – 3224

TROPOSPHERIC – STRATOSPHERIC TIDAL INVESTIGATIONS

HOUGH COMPONENTS OF SURFACE PRESSURE

G. V. Groves and A. Wilson
Department of Physics and Astronomy,
University College London WC1E 6BT
England.

31 August 1981

Final Scientific Report
1 December 1976 – 30 September 1981

Approved for public release; distribution unlimited.

Prepared for:

Air Force Geophysics Laboratory,
L. G. Hanscom Field, Bedford, Massachusetts 01730, USA

European Office of Aerospace Research and Development,
London, England.

REPORT DOCUMENTATION PAGE		READ INSTRUCTIONS BEFORE COMPLETING FORM
1. Report Number AFGL-TR-81-0301	2. Govt Accession No. AD-A106 386	3. Recipient's Catalog Number
4. Title (and Subtitle) TROPOSPHERIC-STRATOSPHERIC INVESTIGATIONS, Hough components of surface pressure		5. Type of Report & Period Covered Part III Final Scientific Report. 1 December 1976-30 September 1981 6. Performing Org. Report Number
7. Author(s) C.V. Groves and A. Wilson		8. Contract or Grant Number AFOSR – 77 – 3224
9. Performing Organization Name and Address Department of Physics and Astronomy, University College London, Gower Street, London WC1E 6BT, England.		10. Program Element, Project, Task Area & Work Unit Numbers 62101F 668705AJ
11. Controlling Office Name and Address Air Force Geophysics Laboratory, L. G. Hanscom AFB, Massachusetts 01731 Monitor/William K. Vickery/LKD		12. Report Date 31 August 1981 13. Number of Pages 50
14. Monitoring Agency Name and Address European Office of Aerospace Research and Development, Box 14, FPO, New York 09510, USA.		15. Unclassified
16. & 17. Distribution Statement Approved for public release; distribution unlimited.		
18. Supplementary Notes		
19. Key Words Atmosphere, oscillations, tides, pressure		
20. Abstract The Report contains two papers. In the first of these, diurnal and semi-diurnal Hough components of surface pressure are evaluated by classical tidal theory for previously presented profiles of water vapour and ozone heating and the values obtained are compared with the observed results of Haurwitz and Cowley (1973). The second paper presents profiles of terdiurnal ozone and water vapour heating from which the corresponding surface pressure oscillations are evaluated by classical tidal theory and compared with earlier evaluations and observationally derived results. In both papers the calculations underpredict the observed values and indicate a need for additional tidal heating to be identified.		

FORM 1473

Diurnal and semi-diurnal Hough components of surface pressure

G. V. Groves
Department of Physics and Astronomy,
University College London,
England

Abstract

Diurnal and semi-diurnal Hough components of surface pressure are evaluated by classical tidal theory for previously presented profiles of water vapour and ozone heating. Values are compared with the observational results of Haurwitz & Cowley (1973) and show significant discrepancies which are considered to indicate the need for additional heating to be identified. The present calculations are in satisfactory agreement with those for semi-diurnal modes evaluated by Walterscheid et al. (1980).

CONTENTS

1. Introduction

Early attention was given to water vapour absorption of solar radiation as a generating source of atmospheric oscillations by Siebert (1961) and likewise for ozone by Butler & Small (1963). Based on these two sources of heating, detailed evaluations of diurnal and semi-diurnal atmospheric tidal fields and surface pressure oscillations have been presented by Lindzen (1967, 1968), Chapman & Lindzen (1970) and Lindzen & Hong (1974).

Using a newly-constructed model of ozone densities, vertical profiles of the diurnal and semi-diurnal Hough modes of ozone heating have been calculated (Groves, 1980a) which differ significantly from those of Chapman & Lindzen (1970) and related papers. In a re-evaluation of the Hough components of water vapour heating (Groves, 1980b) cloud-related scattering properties have been introduced and have the effect of nearly doubling the heating at 8km altitude and of halving it near the surface. In the light of such revisions to the ozone and water vapour heating, the need is apparent for a corresponding evaluation of the atmospheric tidal response.

The present paper deals with surface pressure oscillations generated by the diurnal and semi-diurnal components of ozone and water vapour heating. Calculations are based

on classical tidal theory (Groves, 1981) and for the semi-diurnal component are compared with the evaluations of Walterscheid et al. (1980) which are based on both classical and non-classical assumptions and on revised water vapour and ozone heating rates.

One of the objectives of this paper is to compare calculated values with previously reported observational results. The earlier calculations of Lindzen (1967) for the diurnal tide were found to considerably underpredict the empirical formula of Haurwitz (1965) at latitudes of less than 30° (Chapman & Lindzen, 1970, Fig. 3.26). The analysis of barometric data by Haurwitz & Cowley (1973) has provided a more detailed set of results which offer the possibility of comparing individual diurnal and semi-diurnal Hough components of surface pressure with theoretical values for different seasons. Attention will be confined to modes of oscillation that are independent of longitude, i.e. to migrating modes, as it is for these that observational results are available. Diurnal modes are designated by (1,1,n), or more concisely (1,n); where n = 1, 2, 3,... is a sequence of propagating modes, those with n odd being equatorially symmetric, and n = -1, -2, -3,... is a sequence of trapped modes, those with n even being equatorially symmetric. Semi-diurnal modes are designated by (2,2,n), or more concisely (2,n); where n = 2, 3, 4,... , those with n even being equatorially symmetric.

2. Method of calculation

The surface pressure oscillation of mode (m,n) is expressed in the notation of Groves (1981) as

$$P_s = (P_n^{mR} \cos\sigma t' + P_n^{mI} \sin\sigma t') \Theta_n^m(\theta) \qquad (1)$$

where t' is local time, σ is the angular frequency of the oscillation and Θ_n^m is the corresponding Hough function of colatitude θ. Results are presented in terms of

$$P_n^m = P_n^{mR} + i P_n^{mI} \qquad (2)$$

which is calculated from

$$P_n^m = \ell_P P_J(0) \qquad (3)$$

where $P_J(0)$ is obtained from Equ. 10.14 of Groves (1981) and $\ell_P = p_{oo}\omega_o/\sigma$, p_{oo} being surface pressure and ω_o the Earth's sidereal rate of rotation. Pressure then attains a maximum or minimum value of $|P_n^m|\ \Theta_n^m$ at local time $\sigma^{-1} \tan^{-1}(P_n^{mI}/P_n^{mR})$ according to whether Θ_n^m is positive or negative. The basic atmospheric profiles involved in this calculation are those of the Newtonian cooling constant which will be taken as zero, i.e. all forms of dissipation are then neglected, and the pressure scale height for which the values adopted at 0(2)26 km are

8.75, 8.46, 8.14, 7.82, 7.53, 6.98, 6.63, 6.22, 5.90, 5.99, 6.14, 6.24, 6.39, 6.56 km and at 28(2)150 km are taken from the mean CIRA (1972). The Hough functions introduced in (1) are fully normalized being taken positive at the equator if symmetric and increasing with latitude at the equator if anti-symmetric. Results are presented as plots of P_n^{mI} against P_n^{mR}. Values for the mid-season months of January, April, July and October are numbered 1, 2, 3 and 4 respectively and those from Haurwitz & Cowley (1973), which are for the intervals May to August (J), November to February (D) and the remaining months (E), are qualified by the letters in brackets. Comparisons may therefore be made on an approximate seasonal basis between 1 and D, 2 or 4 and E, and 3 and J. Values are tabulated in terms of amplitude and phase (local time of maximum value) in Tables 1 and 2.

3. Diurnal modes

For diurnal modes, water vapour heating provides a much greater contribution to surface pressure than ozone heating (Table 2). In the case of the trapped sequence of modes, this is a consequence of the trapping of the ozone-generated oscillation at stratospheric-mesospheric heights where air densities are lower and variations have relatively little effect on surface pressure. In the case of propagating

Season		1		2		3		4	
		P	Ph	P	Ph	P	Ph	P	Ph
(1,1)									
	A	290	5.1	283	5.1	255	4.9	283	5.1
	B	231	4.9	245	4.8	208	4.9	241	4.8
(1,-1)									
	A	40	9.9	84	8.0	104	6.7	84	8.0
	B	-	-	-	-	-	-	-	-
(1,-2)									
	A	418	5.1	458	5.3	449	5.5	458	5.3
	B	160	6.0	164	6.0	153	6.0	167	6.0
(1,-4)									
	A	248	5.0	246	5.1	196	4.9	246	5.1
	B	79	6.0	82	6.0	75	6.0	81	6.0
(2,2)									
	A	1100	9.6	1133	9.7	992	9.8	1133	9.7
	B	728	9.0	745	9.0	682	9.0	765	9.0
	C	759	9.0	-	-	759	9.0	-	-
	D	893	9.0	-	-	894	9.0	-	-
(2,3)									
	A	59	9.7	65	0.3	87	1.3	65	0.3
	B	30	2.2	4	8.0	26	8.2	6	2.0
	C	30	2.2	-	-	38	8.4	-	-
	D	55	8.8	-	-	49	2.9	-	-
(2,4)									
	A	166	3.3	182	3.6	151	3.6	182	3.6
	B	22	3.4	28	3.8	22	3.4	30	3.7
	C	16	4.0	-	-	18	3.8	-	-
	D	48	3.7	-	-	51	3.7	-	-

Table 1. Diurnal (m=1) and semidiurnal (m=2) Hough modes of surface pressure amplitude, $P=|P_n^m|$, and phase, Ph, for modes (m,n). A are from Haurwitz and Cowley (1973); B are the present calculations from Table 2 (total); C are the classical and D the non-classical evaluations of Walterscheid et al (1980). Columns 1,2,3,4 refer to the four seasons. In A they are designated D,E,J,E and in C and D seasons 1 and 3 are designated DJF and JJA respectively. In the present calculations, B, they are for January, April, July and October. P is in microbars and Ph is the local time of maximum ($\Theta_n^m > 0$) in hours.

	Water vapour				Ozone				Total			
	P^R	P^I	P	Ph	P^R	P^I	P	Ph	P^R	P^I	P	Ph
(1,1)												
Jan	77	205	219	4.6	-10	16	19	8.2	67	221	231	4.9
Apr	82	212	227	4.6	-9	22	24	7.5	73	234	245	4.8
Jul	70	184	197	4.6	-10	15	18	8.3	60	199	208	4.9
Oct	84	206	223	4.5	-10	23	25	7.5	74	229	241	4.8
(1,-1)												
Jan	0	1	-	-	0	0	-	-	0	1	-	-
Apr	0	0	-	-	0	0	-	-	0	0	-	-
Jul	0	-1	-	-	0	0	-	-	0	-1	-	-
Oct	0	0	-	-	0	0	-	-	0	0	-	-
(1,-2)												
Jan	0	136	136	6.0	0	24	24	6.0	0	160	160	6.0
Apr	0	137	137	6.0	0	27	27	6.0	0	164	164	6.0
Jul	0	130	130	6.0	0	23	23	6.0	0	153	153	6.0
Oct	0	140	140	6.0	0	27	27	6.0	0	167	167	6.0
(1,-4)												
Jan	0	78	78	6.0	0	1	1	6.0	0	79	79	6.0
Apr	0	82	82	6.0	0	0	0	-	0	82	82	6.0
Jul	0	74	74	6.0	0	1	1	6.0	0	75	75	6.0
Oct	0	81	81	6.0	0	0	0	-	0	81	81	6.0

(2,2)												
Jan	2	-248	248	9.0	-9	-480	480	9.0	-7	-728	728	9.0
Apr	2	-261	261	9.0	-9	-484	484	9.0	-7	-745	745	9.0
Jul	2	-233	233	9.0	-8	-449	449	9.0	-6	-682	682	9.0
Oct	2	-267	267	9.0	-9	-498	498	9.0	-7	-765	765	9.0
(2,3)												
Jan	1	1	1	1.5	12	26	29	2.2	13	27	30	2.2
Apr	1	7	7	2.7	-3	-10	10	8.4	-2	-3	4	8.0
Jul	-1	1	1	4.8	-10	-25	27	8.2	-11	-24	26	8.2
Oct	-1	-4	4	8.7	4	9	10	2.3	3	5	6	2.0
(2,4)												
Jan	1	17	17	2.9	-6	4	7	4.9	-5	21	22	3.4
Apr	2	24	24	2.9	-13	1	13	5.8	-11	25	28	3.8
Jul	1	17	17	2.9	-6	4	7	4.8	-5	21	22	3.4
Oct	2	27	27	2.9	-13	1	13	5.8	-11	28	30	3.7

Table 2. Diurnal (m=1) and semidiurnal (m=2) Hough modes of surface pressure evaluated for water vapour heating and ozone heating and modes (m,n). P^R, P^I are the quantities P_n^{mR}, P_n^{mI} defined by (2) and are in microbars. P and Ph are defined in Table 1. The columns under Total are the sum of the water vapour and ozone contributions.

modes, the depth of the heating region in relation to the vertical wavelength of oscillation is important; that of ozone heating being sufficiently great to give rise to surface pressure contributions that tend to cancel.

3.1 Trapped modes

For trapped modes, water vapour and ozone contributions to surface pressure are in phase and their combined values are plotted in Fig 1. For (1,-2) there is a discrepancy between calculated and observed amplitudes of a factor of about 3 and phases differ slightly. Such a large discrepancy is difficult to reconcile with inaccuracies in either observed or calculated values and would seem to imply that water vapour and ozone heating define only a part of the tidal generating source.

The comparisons between observed and calculated values in Fig. 1 for (1,-4) show the same general picture as (1,-2), but some similarity is to be expected as a consequence of the analytical technique and the limited data at high latitudes, where this mode predominates. Of still less independent significance would be comparisons for the (1,-6), (1,-8), (1,-10) modes which are the other modes of this sequence included in the analysis of Haurwitz & Cowley (1973).

A significant asymmetry between the N and S hemispheres

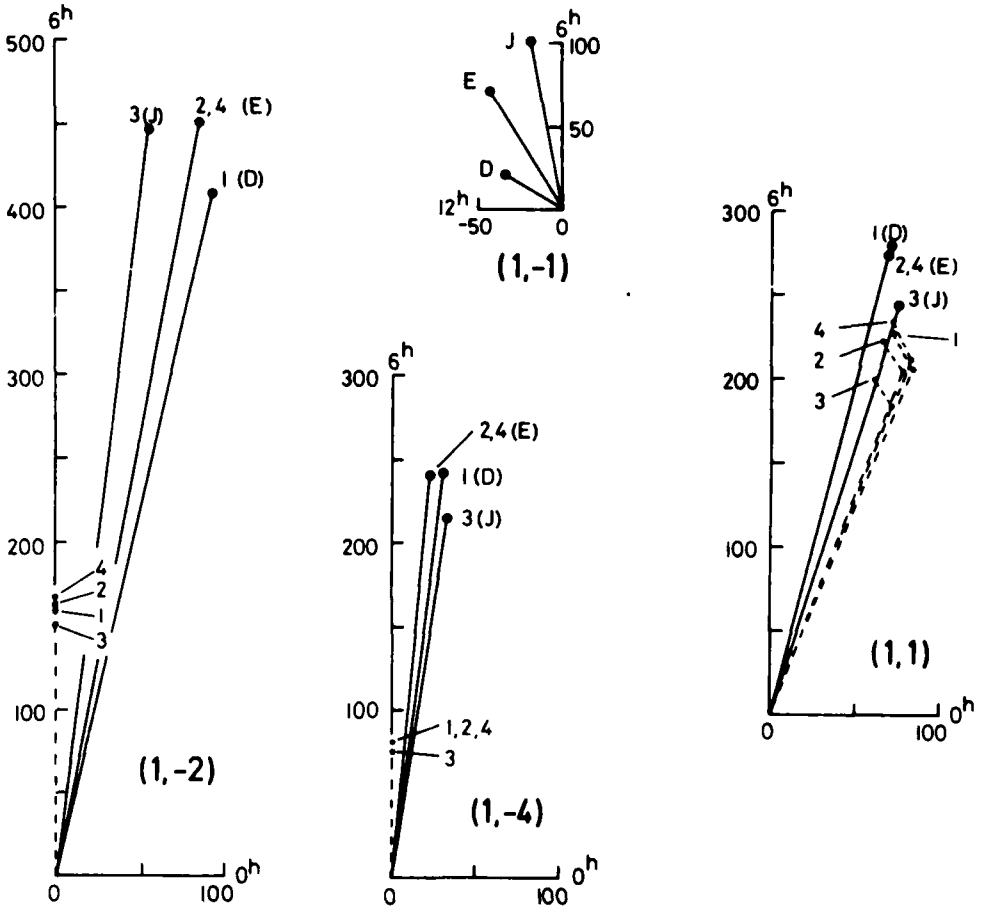

Fig. 1 Diurnal modes. P_n^{mR} and P_n^{mI} are plotted in μb on the horizontal and vertical axes respectively for modes (m,n), m=1, n=1,-1,-2,-4. The local time $\sigma^{-1} \tan^{-1}(P_n^{mI}/P_n^{mR})$ is shown on each axis. 1,2,3,4 denote values for the four seasons. Broken lines are position vectors to calculated values for January, April, July and October. Continuous lines are position vectors to the observationally derived values D, E or J taken from Haurwitz and Cowley (1973).

is apparent in the results of Haurwitz & Cowley (1973) which is represented mainly by the anti-symmetric mode (1,-1) whose values are shown in Fig. 1. No theoretical values are shown for this mode as water vapour and ozone heating generate almost negligible amounts of less than 2 μb. It may be noted that observed values do not decrease to zero with the solar declination but have a significant equinoctial value, E. The only other anti-symmetric mode analysed by Haurwitz & Cowley (1973) is the (1,-3), but few stations exist at latitudes south of 40°S with which to justify its significance as an independent determination.

3.2 Propagating modes

For these modes water vapour and ozone contributions to the surface pressure differ in phase, the ozone contribution being a much smaller one as shown by the dashed lines in Fig. 1 for the (1,1) mode. In contrast to the comparisons made in § 3.1, the (1,1) results show closer agreement between observation and theory: calculated amplitudes are not far short of observed values and there is close agreement in phase; also July amplitudes are slightly smaller in both cases. The (1,3), although analysed by Haurwitz & Cowley (1973), is not included here as the mode predominates at low latitude and it is doubtful whether the density of equatorial stations is adequate to resolve a migrating oscillation of such low-latitude structure.

4. Semi-diurnal modes

The (2,2) mode of surface pressure oscillation commands special attention on account of its large amplitude, which is close to 1000 μb, and its accuracy of better than 100 μb. Following the analysis of Butler & Small (1963), ozone heating has been recognized as its main source of generation. Water vapour generates about half the contribution of ozone heating with the same phase as shown in Fig. 2. Discrepancies between observation and theory are apparent in Fig. 2 in both the amplitude and phase of (2,2), but earlier classical evaluations, such as that indicated in Fig. 2 by L (Lindzen, 1968), have shown agreement in amplitude to be very good and it has been the discrepancy in phase that has previously attracted attention (Lindzen & Blake, 1971; Lindzen, 1978). The reduced (2,2) amplitude of the present calculations is supported by the classical evaluations of Walterscheid et al. (1980) for the solstices which are marked by W_C in Fig. 2. Walterscheid et al. (1980) also evaluate surface pressure modes under non-classical assumptions, account being taken of mean zonal winds and meridional temperature gradients, and obtain the increased (2,2) amplitude marked by W_N in Fig. 2. This value still underpredicts the observed solstitial values by 10% and 20% respectively, and notably

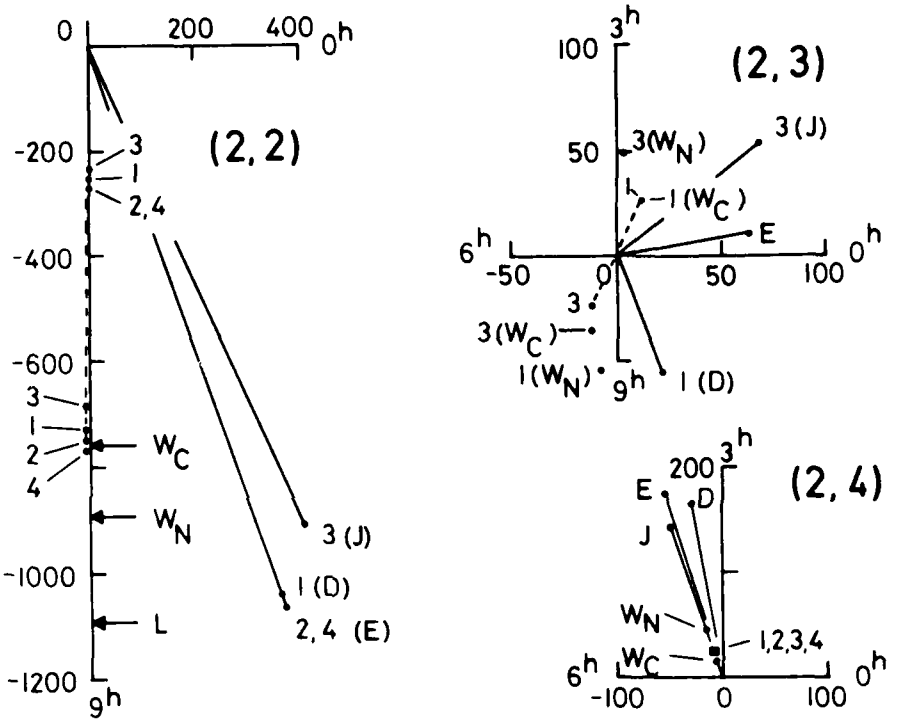

Fig. 2 Semi-diurnal modes. As for Fig. 1 with m=2, n=2,3,4. Note the change of scale between graphs. L denotes value from Lindzen (1968). W_C, W_N are the classical and non-classical values from Walterscheid et al. (1980).

does nothing to reduce the discrepancy in phase.

For the (2,4) mode, calculated values fall within the filled-in square in Fig. 2 for all four seasons and are in fairly good agreement with the classically derived solstitial values of Walterscheid et al. (1980) which are marked by W_C. Such values agree with the phase of the observed E, J and D values but have only a fraction of their amplitude. Larger amplitudes have been obtained by the non-classical calculations of Walterscheid et al. (1980), as shown at W_N in Fig. 2, but these are still only about a third of those observed. Values for (2,5) and (2,6) have been presented by Haurwitz & Cowley (1973), but no comparisons with calculation are made here on account of the limited data available at high latitudes. Results are however presented in Fig. 2 for the leading anti-symmetric mode (2,3) at the solstices for which there is very good agreement between the January values calculated here and that of Walterscheid et al. (1980), denoted respectively by 1 and $1(W_C)$ in Fig. 2, and likewise for the July values denoted respectively by 3 and $3(W_C)$. These pairs of values are in opposite quadrants corresponding to the reversal of sign of the solar declination. The observed values do not however decrease to zero with solar declination but have the equinoctial mean, E. Non-classical (2,3) results denoted by $1(W_N)$, $3(W_N)$ differ appreciably from the classical ones $1(W_C)$, $3(W_C)$; and are in substantially better agreement with observation.

5. Discussion

For diurnal and semi-diurnal frequencies comparisons have been made between Hough modes of surface pressure calculated for water vapour and ozone heating and the observational results of Haurwitz & Cowley (1973). The accuracies of the latter suffer to some unknown extent from the uneven distribution of observing stations which are mainly concentrated in land areas at mid-latitudes. Accordingly, comparisons between calculated and observed values need to be interpreted with caution, and comparisons have not been included in this paper for some of the modes treated in the Haurwitz & Cowley (1973) analysis which predominate at high latitudes where data are sparse. The determination of migrating diurnal modes is particularly affected by the station distribution as local and migrating parts of diurnal oscillations are of comparable magnitude, whereas for the semi-diurnal oscillation this is not the case, the migrating part being dominant. For this reason, the underprediction at low latitudes of Haurwitz's (1965) empirical formula for the diurnal oscillation (Chapman & Lindzen, 1970, Fig. 3.26) was previously attributed to the likely inaccuracy of determination of the migrating diurnal oscillation at low latitudes where station density is low (Chapman & Lindzen, 1970, p. 170). From the comparisons of the present paper in terms of modes (Fig. 1), theory and observation are in

quite close agreement for the low-latitude confined (1,1) mode, whereas serious underprediction by a factor of nearly 3 arises with the (1,-2) mode. It is not clear why the underprediction should be associated mainly with the (1,-2). One possibility is that a source of tidal generation additional to the adopted water vapour and ozone heating is present with a latitudinal distribution that contributes substantially to (1,-2) and relatively little to (1,1). If, however, the earlier appeal to low station density is followed, the limitations would have to be at high latitudes where (1,-2) predominates and (1,1) is inconsequential and not at low latitudes as previously suggested. In this case, some 2/3 of the observed (1,-2) mode would need to be attributed to inadequately resolved non-migrating modes, i.e. (1,s,-2) with s taking values close to 1; and the problem of identifying an additional source of tidal generation would still remain.

For the (1,-1) mode, water vapour and ozone heating provide negligible contributions to surface pressure and again the possibility of an additional tidal source attracts attention. In the case of this mode, which is anti-symmetric, the limited distribution of S hemisphere stations causes concern about the accuracy with which migrating and non-migrating oscillations can be resolved so that what was analysed and identified as (1,-1) may actually be a

lumped set of modes (1,s,-1), s taking values near to 1. Even so, the source of excitation of such modes still needs to be identified.

The (2,2) is the largest tidal mode of surface pressure and, on account of the global regularity of the semi-diurnal oscillation, is the best observationally determined mode. The discrepancy between observation and theory, amounting to about 400 μb in P_2^{2R} (Fig. 2), must therefore be considered a serious shortcoming in the application of tidal theory. The problem has been considered at some length by Lindzen & Blake (1971) who showed that neither dissipation, surface heating nor mean winds could provide an answer. A later analysis (Lindzen, 1978) supported the suggestion that the discrepancy may be due to the release of the latent heat of a semi-diurnal oscillation in tropical rainfall, although the origin of the oscillation in rainfall remained unaccounted for. In view of the magnitude of the discrepancy in (2,2), a discrepancy in (2,4) of the magnitude shown in Fig. 2 is not entirely unexpected.

The observational (2,3) results have a similar characteristic to those of the (1,-1) in that the equinoctial mode does not vanish as would happen if the heating asymmetry depended solely on solar declination. Also like the (1,-1),

observational data from the S hemisphere may be so sparse that the results actually represent a lumped set of modes, being in this case (2,s,3), where s takes values near to 2.

The evaluations of Walterscheid et al. (1980) of semi-diurnal modes by classical theory are denoted by W_C in Fig. 2 and show satisfactory agreement with the present calculations. The effect of introducing non-classical assumptions was examined by Walterscheid et al. (1980) and the results obtained, which are denoted by W_N in Fig. 2, are closer to the observational ones, the improvement being quite substantial for (2,3). Significant discrepancies still however remain between observation and theory as discussed above and indicate the need for additional heating to be identified.

Acknowledgements - Sponsorship has been provided for this work by the Air Force Geophysics Laboratory (AFGL), United States Air Force under Grant No. AFOSR - 77 - 3224. The assistance of Mr. Jonathan D. Groves with data preparation and computer processing on the GEC 4082 machines (EUCLID) at University College London is very gratefully acknowledged.

REFERENCES

BUTLER, S.T. & SMALL, K.A. (1963) Proc. R. Soc. Lond. A274, 91-121.

CHAPMAN, S. & LINDZEN, R.S. (1970) Atmospheric tides: thermal and gravitational. Dordrecht, Holland, D. Reidel Publishing Co.

CIRA (1972) COSPAR International Reference Atmosphere 1972, Akademie-Verlag, Berlin.

GROVES, G.V. (1980a) Hough components of ozone heating, in Interim Scientific Report No. 4, AFOSR-77-3224, Department of Physics and Astronomy, University College London, Gower Street, London WC1E 6BT, England, 30 June 1980.

GROVES, G.V. (1980b) Hough components of water vapour heating, in Final Scientific Report, Part I, AFOSR-77-3224, Department of Physics and Astronomy, University College London, Gower Street, London WC1 6BT, England, 31 December 1980.

GROVES, G.V. (1981) The vertical structure of atmospheric oscillations formulated by classical tidal theory, in Final Scientific Report, Part II, AFOSR-77-3224, Department of Physics and Astronomy, University College London, Gower Street, London WC1E 6BT, England, 28 February 1981.

HAURWITZ, B. (1965) Archiv. Meteorol. Geophys. Biokl. A14, 361-379.

HAURWITZ, B. & COWLEY, A.D. (1973) Pure Appl. Geophys. 102, 193-221.

LINDZEN, R.S. (1967) Quart. J. R. Met. Soc. 93, 18-42.

LINDZEN, R.S. (1968) Proc. R. Soc. Lond. A303, 299-316.

LINDZEN, R.S. (1978) Mon. Wea. Rev. 106, 526-533.

LINDZEN, R.S. & BLAKE, D. (1971) Geophys. Fl. Dyn. 2, 31-61.

LINDZEN, R.S. & HONG, S-S. (1974) J. Atmos. Sci. 31, 1421-1446.

SIEBERT, M. (1961) Adv. Geophys. 7, 105-182.

WALTERSCHEID, R.L., DeVORE, J.G. & VENKATESWARAN, S.V. (1980) J. Atmos. Sci. 37, 455-470.

Terdiurnal Hough components of surface pressure

A. Wilson and G. V. Groves
Department of Physics and Astronomy,
University College London,
England

Abstract

Profiles of terdiurnal heating due respectively to ozone and water vapour absorption of solar radiation are calculated for the (3,3,3) to (3,3,6) Hough modes and corresponding surface pressure oscillations are evaluated by classical tidal theory. Comparisons are made with earlier evaluations and with observationally derived results. The calculated solstitial (3,3,4) mode, which is the mode of largest surface pressure amplitude, shows good agreement in phase with observation but underpredicts observed amplitudes by about 36 per cent in contrast to earlier evaluations which were based on a now unacceptable basic temperature profile.

CONTENTS

1. Introduction

Hann (1918) first described the terdiurnal component of surface pressure, its main characteristics being that it undergoes a 180° phase change between summer and winter and its amplitude tends to zero at the equinoxes. Following Siebert's (1961) investigation of the tidal effects of the insolation of water vapour, Butler & Small (1963) carried out a similar investigation for ozone and concluded that nearly all of the terdiurnal variation of surface pressure could be accounted for by these two sources of heating. Since then the terdiurnal atmospheric tide has received little attention although the temperature profiles used in the earlier analyses have been modified in the light of new data and more detailed water vapour and ozone models are now available. A re-evaluation of the terdiurnal surface pressure therefore seems to be in order.

The present paper calculates Hough functions for the (3,3,3) to (3,3,6) modes and presents their form graphically; the relevant heating components for ozone and water vapour are computed; the surface pressure oscillations arising from this heating are calculated and comparisons are made with previous predictions and observed results. The work is an extension of that on diurnal and semidiurnal heating (Groves, 1980a,b) and corresponding surface pressures (Groves, 1981).

2. Terdiurnal Hough functions

The calculation of Hough functions has been described previously in detail (Groves, 1979). The eigenvectors $\{a_r\}$ corresponding to the eigenvalues λ of a matrix whose elements depend on the Hough mode are found and the Hough functions Θ are obtained from

$$\Theta = \sum_{r=s}^{\infty} a_r P_{r,s}(\mu)$$

where μ = cos(colatitude), s is the number of wavelengths that fit a circle of latitude and $P_{r,s}$ is the normalized associated Legendre function.

The matrix can, for ease of calculation, be divided into two symmetrical matrices, one producing eigenvectors $(a_s, 0, a_{s+2}, 0, \ldots)$ and the other $(a_{s+1}, 0, a_{s+3}, 0, \ldots)$. These eigenvectors are then normalized by dividing by $(a_s^2 + a_{s+2}^2 + \ldots)^{1/2}$ and $(a_{s+1}^2 + a_{s+3}^2 + \ldots)^{1/2}$ respectively. Values of equivalent depths obtained from $h = \lambda/0.011349$ km for modes (3,3,n), n = 3, . . 8, are 12.890, 7.662, 5.085, 3.624, 2.714 and 2.109 km respectively. These values agree with those which were given by Siebert (1961) to one less significant figure for n = 3,. . . 7. The following series expansions are obtained for migrating modes, i.e. for s = 3:

$$\Theta_3^3 = 0.9965\, P_{3,3} - 0.0837\, P_{5,3} + 0.3571\times10^{-2}\, P_{7,3} - 0.8807\times10^{-4}\, P_{9,3} + \ldots$$

$$\Theta_4^3 = 0.9907\, P_{4,3} - 0.1355\, P_{6,3} + 0.8401\times10^{-2}\, P_{8,3} - 0.3025\times10^{-3}\, P_{10,3} + \ldots$$

$$\Theta_5^3 = 0.0830\, P_{3,3} + 0.9798\, P_{5,3} - 0.1813\, P_{7,3} + 0.0148\, P_{9,3} - 0.7077\times10^{-3}\, P_{11,3} + \ldots$$

$$\Theta_6^3 = 0.1339\, P_{4,3} + 0.9652\, P_{6,3} - 0.2233\, P_{8,3} + 0.0226\, P_{10,3} - \ldots$$

Comparison of the coefficients with Siebert (1961) has to be made with the aid of the relation

$$P_n^m = \left[2/(2n+1)^{1/2}\right] P_{n,m} \qquad m > 0$$

$$= \left[2/(2n+1)\right]^{1/2} P_{n,m} \qquad m = 0$$

since Siebert used the seminormalized Schmidt form P_n^m. The two sets of coefficients are found to be in agreement. Table 1 shows the comparison for the (3,3,4) mode. The forms of the (3,3,3) to (3,3,6) Hough functions are shown in Fig. 1. Signs are chosen so that the symmetric functions (3,3,3) and (3,3,5) are positive at the equator and the antisymmetric functions increase with latitude at the equator going north. (3,3,3) is the only wholly-positive terdiurnal Hough function.

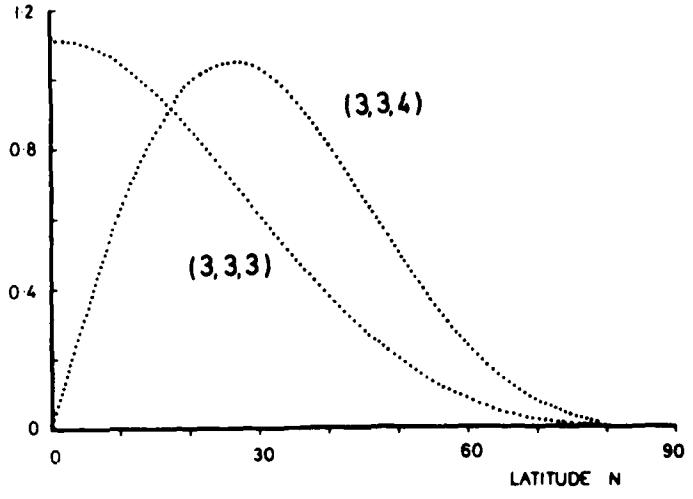

Fig. 1. Terdiurnal Hough functions; above for (3,3,3) and (3,3,4), below for (3,3,5) and (3,3,6).

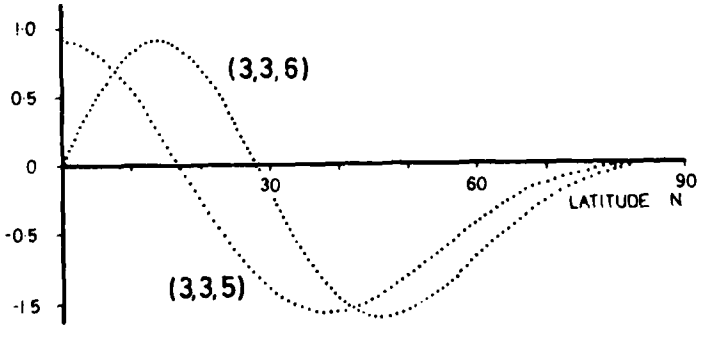

3. Ozone heating

The calculations are based on methods and models described previously (Groves, 1980a). The ozone model originally extended to $\pm 60^{\circ}$ latitude and 75 km height (Lucas, 1978) and was derived from ground, rocket and satellite measurements. Extensions to $\pm 90^{\circ}$ and 80 km were then added using provisional values. Surface albedo values of 0.07, 0.14, 0.21 or 0.75 were assigned to 10° latitude x 10° longitude areas on the basis of all sea, all land, half sea and half land or snow cover. No daily or seasonal variations of surface albedo were included. Cloud albedoes of 0.25, 0.625 or 0.875 were given to 10° latitude x 10° longitude areas on a seasonal basis. These models were also used in the calculation of water vapour heating, results of which are given in § 4.

Table 1. Series coefficients for the (3,3,4) Hough function

	Eigenvector	$\frac{2}{(2n+1)^{\frac{1}{2}}}$	Siebert's coefficients	a_r corrected to Siebert's form
a_4	0.99074	0.66667	1	1
a_6	-0.13551	0.55470	-0.164	-0.1644
a_8	0.00840	0.48507	0.012	0.0117
a_{10}	-0.00030	0.43644	-0.0005	-0.0005

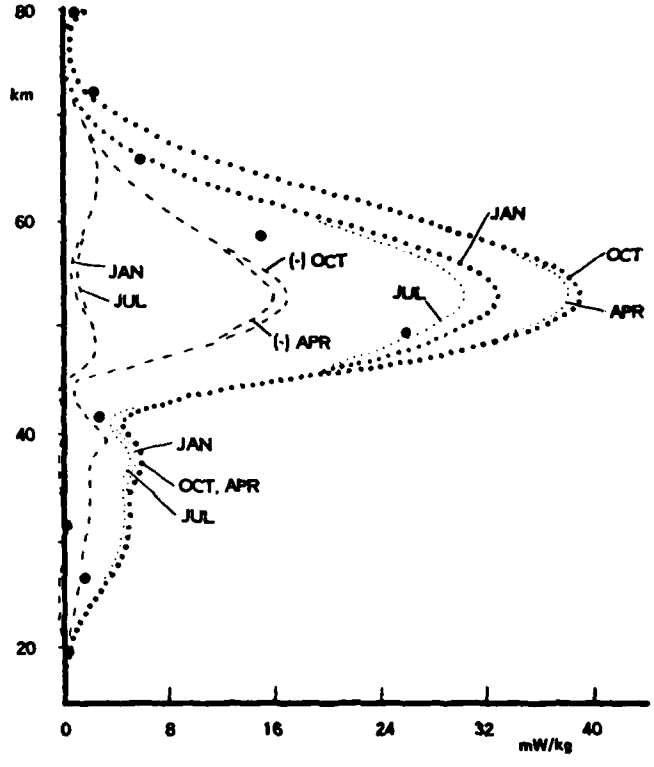

Fig. 2. Height profiles of Hough components of ozone heating for two modes. Key: .....(3,3,3); -----(3,3,5). Butler and Small (1963) spring equinox values are denoted by • for (3,3,3).

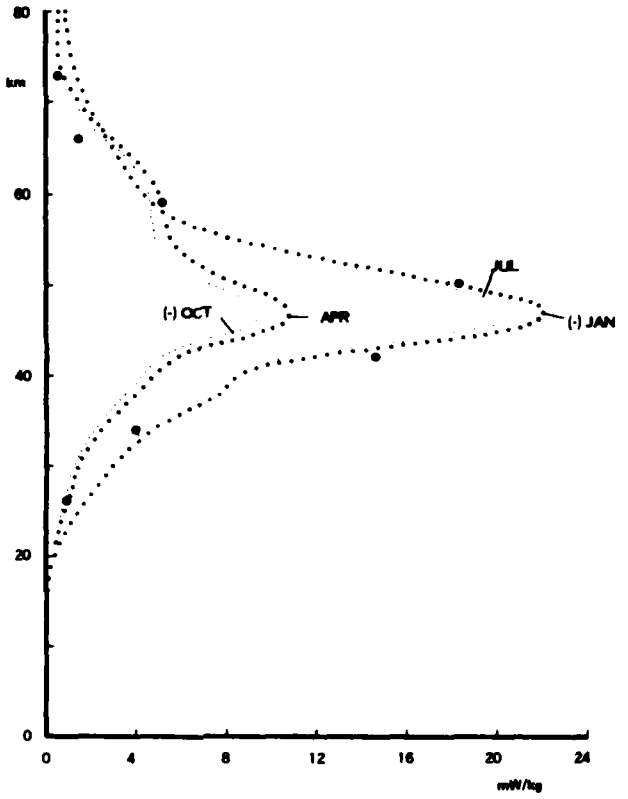

Fig. 3. Height profile of the (3,3,4) Hough component of ozone heating. Butler and Small (1963) summer solstice values are denoted by ●.

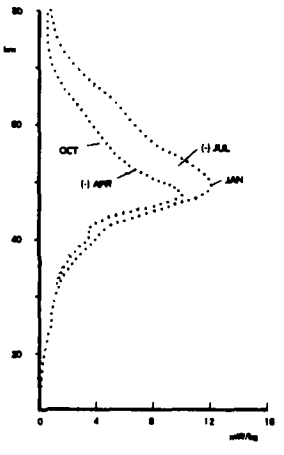

Fig. 4. Height profile of the (3,3,6) Hough component of ozone heating.

H	(3,3,3)				(3,3,4)			
km	mW/kg				mW/kg			
	Jan	Apr	Jul	Oct	Jan	Apr	Jul	Oct
0	0.0	0.0	0.0	0.0	-0.0	0.0	0.0	-0.0
2	0.0	0.0	0.0	0.0	-0.0	0.0	0.0	-0.0
4	0.0	0.0	0.0	0.0	-0.0	0.0	0.0	-0.0
6	0.0	0.0	0.0	0.0	-0.0	0.0	0.0	-0.0
8	0.0	0.0	0.0	0.0	-0.0	0.0	0.0	-0.0
10	0.0	0.1	0.0	0.1	-0.0	0.0	0.0	-0.0
12	0.0	0.1	0.0	0.1	-0.0	0.0	0.0	-0.0
14	0.0	0.1	0.0	0.1	-0.1	0.1	0.1	-0.1
16	0.1	0.1	0.1	0.1	-0.1	0.1	0.1	-0.1
18	0.1	0.3	0.1	0.3	-0.2	0.2	0.2	-0.2
20	0.4	0.7	0.4	0.7	-0.4	0.3	0.4	-0.3
22	1.0	1.3	0.9	1.3	-0.7	0.5	0.7	-0.4
24	1.9	2.2	1.7	2.2	-1.2	0.7	1.2	-0.6
26	3.0	3.3	2.8	3.3	-1.8	1.0	1.7	-0.9
28	4.1	4.1	3.8	4.2	-2.4	1.2	2.3	-1.1
30	4.8	4.6	4.4	4.7	-3.0	1.5	2.8	-1.4
32	5.1	4.9	4.7	5.0	-3.7	2.0	3.6	-1.7
34	5.0	5.0	4.7	5.1	-4.7	2.5	4.5	-2.2
36	5.1	5.3	4.7	5.4	-6.1	3.2	5.8	-2.9
38	5.6	5.8	5.1	5.9	-7.8	4.1	7.4	-3.6
40	4.3	4.7	4.0	4.8	-8.5	4.8	8.1	-4.3
42	4.4	4.8	4.1	4.9	-11.6	5.8	11.0	-5.2
44	10.4	10.4	9.6	10.7	-15.0	8.5	17.0	-7.5
46	18.6	19.8	17.2	20.2	-21.9	10.6	20.6	-9.4
48	25.6	28.9	23.7	29.6	-21.3	10.5	20.2	-9.1
50	29.6	34.7	27.5	35.5	-17.9	8.6	17.0	-7.4
52	32.3	37.8	30.0	38.6	-13.8	6.9	13.1	-5.9
54	32.5	38.0	30.2	38.8	-10.8	5.8	9.6	-5.0
56	30.6	36.2	28.4	36.9	-7.1	5.4	6.8	-4.8
58	26.4	32.5	24.5	33.1	-5.5	5.2	5.2	-4.7
60	21.3	27.6	19.5	28.1	-4.3	5.0	4.2	-4.6
62	14.9	21.9	13.8	22.3	-3.7	4.5	3.6	-4.2
64	9.3	16.3	9.1	16.6	-3.2	3.9	3.2	-3.6
66	6.0	11.1	5.6	11.3	-2.7	2.9	2.6	-2.7
68	3.5	7.0	3.2	7.1	-2.2	2.1	2.1	-1.9
70	1.8	4.0	1.7	4.1	-1.8	1.4	1.7	-1.3
72	0.8	1.9	0.7	1.9	-1.5	0.9	1.4	-0.8
74	0.3	0.9	0.3	0.9	-1.3	0.7	1.2	-0.6
76	0.1	0.5	0.1	0.5	-1.1	0.5	1.0	-0.5
78	1.2	0.6	0.2	0.6	-0.9	0.5	0.9	-0.5
80	1.0	1.8	0.2	1.9	-0.9	0.7	0.9	-0.6

Table 2. Hough components of ozone heating associated with modes (3,3,3) to (3,3,6).

/continued

h	(3,3,5)				(5,3,6)			
km	mW/kg				mW/kg			
	Jan	Apr	Jul	Oct	Jan	Apr	Jul	Oct
0	-0.0	-0.0	-0.0	-0.0	0.0	-0.0	-0.0	0.0
2	-0.0	-0.0	-0.0	-0.0	0.0	-0.0	-0.0	0.0
4	-0.0	-0.0	-0.0	-0.0	0.0	-0.0	-0.0	0.0
6	-0.0	-0.0	-0.0	-0.0	0.0	-0.0	-0.0	0.0
8	-0.0	-0.0	-0.0	-0.0	0.0	-0.0	-0.0	0.0
10	-0.0	-0.1	-0.0	-0.1	0.0	-0.0	-0.0	0.0
12	-0.0	-0.1	-0.0	-0.1	0.1	-0.1	-0.1	0.1
14	-0.0	-0.1	0.0	-0.1	0.1	-0.1	-0.1	0.1
16	-0.0	-0.2	0.0	-0.2	0.1	-0.1	-0.1	0.1
18	-0.0	-0.3	-0.0	-0.3	0.2	-0.2	-0.2	0.2
20	-0.1	-0.5	-0.1	-0.5	0.4	-0.3	-0.3	0.3
22	-0.2	-0.7	-0.1	-0.7	0.5	-0.5	-0.5	0.4
24	-0.2	-1.0	-0.1	-1.0	0.7	-0.6	-0.6	0.5
26	-0.1	-1.2	-0.1	-1.3	0.8	-0.7	-0.8	0.7
28	-0.1	-1.4	0.0	-1.5	1.0	-0.9	-0.9	0.8
30	-0.0	-1.6	0.1	-1.7	1.2	-1.0	-1.1	0.9
32	-0.1	-1.8	0.0	-2.0	1.4	-1.2	-1.5	1.1
34	-0.2	-2.0	-0.1	-2.1	1.8	-1.5	-1.7	1.4
36	-0.2	-2.0	-0.1	-2.1	2.4	-1.9	-2.2	1.7
38	-0.2	-2.2	-0.1	-2.4	3.2	-2.6	-3.0	2.4
40	0.1	-2.9	0.2	-3.1	4.0	-3.5	-3.7	3.1
42	-0.1	-1.5	-0.1	-1.7	4.7	-3.6	-4.4	3.2
44	-0.2	-0.9	-0.2	-1.0	7.0	-5.3	-6.5	4.8
46	1.2	-3.7	1.2	-4.0	9.7	-8.5	-9.0	7.6
48	2.5	-8.8	2.6	-9.6	11.7	-9.9	-10.8	8.8
50	2.4	-13.2	2.6	-14.3	12.0	-8.6	-11.1	7.5
52	1.5	-15.5	1.8	-16.7	11.1	-6.8	-10.2	5.9
54	0.9	-15.4	1.5	-16.5	9.7	-5.6	-9.0	5.0
56	0.8	-13.7	1.2	-14.6	8.3	-4.9	-7.8	4.4
58	1.3	-11.2	1.6	-11.9	7.3	-4.3	-6.9	4.0
60	1.9	-8.7	2.2	-9.2	6.6	-3.7	-6.3	3.5
62	2.5	-6.6	2.5	-6.9	5.9	-3.1	-5.7	2.9
64	2.7	-4.8	2.8	-5.1	5.2	-2.5	-5.0	2.3
66	2.6	-3.3	2.6	-3.5	4.3	-1.8	-4.1	1.7
68	2.2	-2.1	2.2	-2.3	3.3	-1.3	-3.2	1.2
70	1.8	-1.3	1.7	-1.4	2.5	-0.9	-2.4	0.9
72	1.4	-0.7	1.3	-0.7	1.9	-0.7	-1.8	0.6
74	1.1	-0.3	1.0	-0.4	1.4	-0.6	-1.3	0.5
76	0.8	-0.1	0.7	-0.2	1.1	-0.5	-1.0	0.5
78	0.6	-0.2	0.5	-0.2	0.9	-0.5	-0.8	0.5
80	0.3	-0.7	0.3	-0.7	0.8	-0.6	-0.7	0.5

Table 2 (continued).

Hough components of ozone heating were calculated from Equ. 3.21 of Groves (1980a) and are presented in Figs. 2 to 4 and Table 2 for the (3,3,3) to (3,3,6) modes. In all cases maximum heating occurs around 50 km. For the (3,3,3) mode the July maximum is some 6.5 per cent less than January's, in keeping with the increased solar distance. For the (3,3,4) mode the peak July heating is 1.7 times that of April being mainly dependent on solar declination which is 9^{o} for the April calculation.

For purposes of comparison, the values obtained by Butler & Small (1963) are shown in Figs. 2 and 3. The Butler & Small (1963) values are generally lower than the present values for (3,3,3); but their points for (3,3,4) in July are in good agreement with the present curves.

4. Water vapour heating

Hough components of water vapour heating are calculated by Equ. 6.9 of Groves (1980b) and include the effect of scattering by clouds. The cloud and surface albedo models are those used in the ozone heating analysis, and the humidity model was based on the maps of Newell et al. (1972) for January, April, July and October at 1000, 700, 500 and 400 mb.

The water vapour heating profiles are presented in Figs. 5 to 7 and Table 3. All of the maxima occur at around

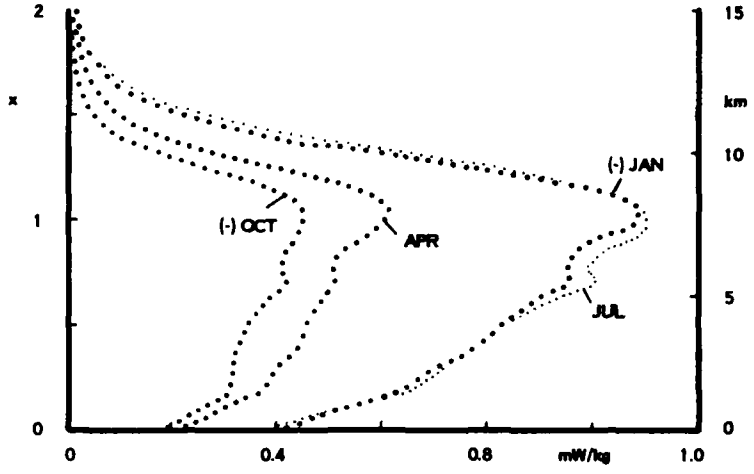

Fig. 5. Height profile of the (3,3,4) Hough component of water vapour heating. x is the natural log of the pressure ratio. An approximate height scale is given on the right.

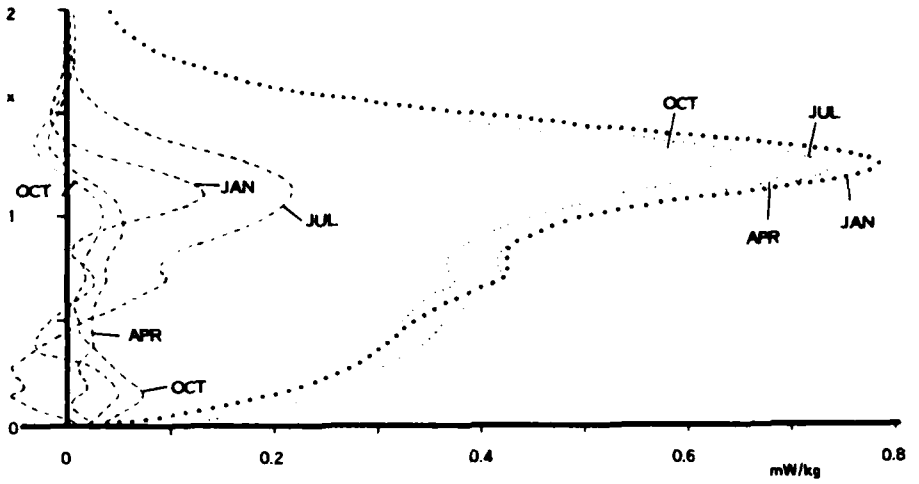

Fig. 6. Height profiles of Hough components of water vapour heating for two modes. Key: .....(3,3,3); ----- (3,3,5).

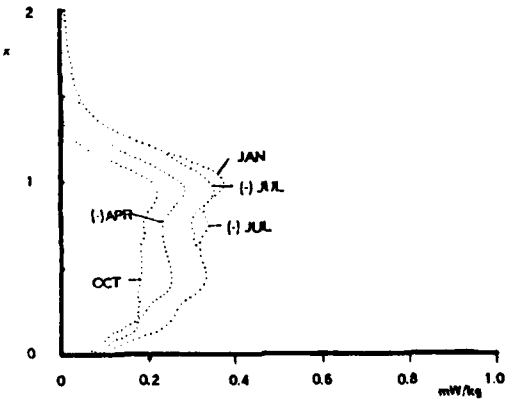

Fig. 7. Height profile of the (3,3,6) Hough component of water vapour heating.

x	(3,3,3) mW/kg				(3,3,4) mW/kg			
	Jan	Apr	Jul	Oct	Jan	Apr	Jul	Oct
0.00	0.02	0.06	0.05	0.04	-0.39	0.20	0.36	-0.17
0.05	0.10	0.15	0.09	0.12	-0.46	0.25	0.44	-0.21
0.10	0.15	0.20	0.12	0.17	-0.51	0.29	0.50	-0.25
0.15	0.20	0.24	0.15	0.22	-0.59	0.34	0.59	-0.29
0.20	0.23	0.27	0.18	0.25	-0.64	0.37	0.65	-0.31
0.25	0.26	0.29	0.20	0.27	-0.67	0.38	0.68	-0.31
0.30	0.28	0.30	0.22	0.28	-0.70	0.40	0.71	-0.31
0.35	0.29	0.33	0.24	0.29	-0.75	0.42	0.75	-0.31
0.40	0.31	0.34	0.26	0.30	-0.78	0.44	0.78	-0.32
0.45	0.32	0.35	0.27	0.31	-0.80	0.45	0.80	-0.33
0.50	0.33	0.36	0.29	0.32	-0.83	0.46	0.83	-0.34
0.55	0.35	0.37	0.31	0.33	-0.85	0.47	0.86	-0.36
0.60	0.37	0.39	0.34	0.34	-0.88	0.48	0.90	-0.37
0.65	0.39	0.40	0.37	0.36	-0.91	0.49	0.95	-0.39
0.70	0.42	0.43	0.40	0.37	-0.95	0.51	1.00	-0.41
0.75	0.42	0.42	0.40	0.37	-0.95	0.50	1.00	-0.41
0.80	0.42	0.41	0.41	0.36	-0.95	0.51	1.00	-0.41
0.85	0.43	0.42	0.42	0.37	-0.97	0.52	1.02	-0.41
0.90	0.44	0.44	0.45	0.39	-1.01	0.55	1.06	-0.43
0.95	0.46	0.47	0.48	0.42	-1.06	0.58	1.09	-0.44
1.00	0.50	0.50	0.51	0.44	-1.08	0.60	1.10	-0.45
1.05	0.55	0.54	0.54	0.48	-1.08	0.61	1.08	-0.44
1.10	0.63	0.59	0.60	0.52	-1.05	0.59	1.05	-0.43
1.15	0.70	0.64	0.66	0.56	-0.98	0.54	1.00	-0.39
1.20	0.76	0.68	0.71	0.60	-0.88	0.47	0.92	-0.33
1.25	0.78	0.70	0.74	0.63	-0.75	0.38	0.82	-0.26
1.30	0.75	0.68	0.71	0.61	-0.62	0.30	0.70	-0.20
1.35	0.68	0.62	0.65	0.57	-0.49	0.23	0.57	-0.14
1.40	0.59	0.54	0.56	0.50	-0.38	0.17	0.45	-0.10
1.45	0.49	0.46	0.47	0.42	-0.29	0.13	0.35	-0.07
1.50	0.39	0.37	0.37	0.34	-0.21	0.09	0.26	-0.04
1.55	0.30	0.29	0.29	0.27	-0.16	0.07	0.19	-0.03
1.60	0.23	0.23	0.22	0.20	-0.12	0.06	0.14	-0.02
1.65	0.18	0.13	0.17	0.16	-0.09	0.04	0.10	-0.02
1.70	0.14	0.14	0.13	0.12	-0.06	0.03	0.08	-0.01
1.75	0.11	0.11	0.10	0.10	-0.05	0.03	0.06	-0.01
1.80	0.09	0.09	0.08	0.08	-0.04	0.02	0.04	-0.01
1.85	0.07	0.07	0.06	0.06	-0.03	0.02	0.04	-0.01
1.90	0.05	0.06	0.05	0.05	-0.02	0.02	0.03	-0.01
1.95	0.05	0.05	0.04	0.04	-0.02	0.01	0.02	-0.01
2.00	0.04	0.04	0.03	0.04	-0.02	0.01	0.02	-0.00

Table 3. Hough components of water vapour heating associated with modes (3,3,3) to (3,3,6).

/continued

x	(3,3,5) m²/kg				(3,3,6) m²/kg			
	Jan	Apr	Jul	Oct	Jan	Apr	Jul	Oct
0.00	-0.02	-0.03	-0.02	-0.02	0.06	-0.06	-0.08	0.07
0.05	-0.03	-0.02	0.01	-0.04	0.14	-0.09	-0.14	0.11
0.10	-0.04	-0.00	0.04	-0.06	0.19	-0.11	-0.18	0.14
0.15	-0.05	-0.00	0.05	-0.07	0.23	-0.14	-0.23	0.18
0.20	-0.05	-0.02	0.04	-0.07	0.26	-0.13	-0.26	0.19
0.25	-0.04	-0.01	0.05	-0.05	0.27	-0.19	-0.28	0.19
0.30	-0.02	-0.01	0.05	-0.04	0.28	-0.21	-0.29	0.18
0.35	-0.02	-0.02	0.04	-0.02	0.31	-0.24	-0.32	0.18
0.40	0.03	-0.02	0.02	-0.01	0.33	-0.25	-0.33	0.18
0.45	0.03	-0.02	0.01	-0.01	0.33	-0.25	-0.33	0.18
0.50	0.02	-0.02	-0.01	-0.01	0.33	-0.25	-0.33	0.19
0.55	0.01	-0.03	-0.03	-0.01	0.33	-0.25	-0.32	0.19
0.60	-0.01	-0.03	-0.06	-0.01	0.32	-0.24	-0.32	0.19
0.65	-0.02	-0.03	-0.08	-0.01	0.31	-0.23	-0.33	0.19
0.70	-0.03	-0.04	-0.09	-0.02	0.31	-0.23	-0.34	0.19
0.75	-0.02	-0.04	-0.09	-0.02	0.30	-0.23	-0.33	0.19
0.80	-0.01	-0.04	-0.09	-0.02	0.31	-0.24	-0.33	0.20
0.85	-0.00	-0.04	-0.11	-0.02	0.32	-0.26	-0.33	0.21
0.90	-0.01	-0.05	-0.14	-0.03	0.35	-0.28	-0.35	0.22
0.95	-0.04	-0.05	-0.17	-0.03	0.37	-0.28	-0.35	0.22
1.00	-0.07	-0.05	-0.19	-0.03	0.37	-0.27	-0.34	0.21
1.05	-0.11	-0.05	-0.21	-0.03	0.36	-0.24	-0.32	0.18
1.10	-0.13	-0.04	-0.21	-0.03	0.32	-0.21	-0.29	0.15
1.15	-0.15	-0.03	-0.21	-0.01	0.27	-0.16	-0.25	0.09
1.20	-0.10	-0.02	-0.20	0.00	0.21	-0.13	-0.21	0.05
1.25	-0.07	0.00	-0.16	0.02	0.16	-0.10	-0.18	0.02
1.30	-0.04	0.01	-0.15	0.03	0.12	-0.08	-0.14	0.01
1.35	-0.01	0.02	-0.12	0.03	0.09	-0.07	-0.11	0.00
1.40	0.01	0.02	-0.09	0.03	0.07	-0.06	-0.09	0.00
1.45	0.01	0.01	-0.06	0.02	0.05	-0.05	-0.07	0.00
1.50	0.01	0.01	-0.04	0.02	0.04	-0.04	-0.05	0.00
1.55	0.01	0.00	-0.03	0.01	0.03	-0.03	-0.04	0.00
1.60	0.01	0.01	-0.02	0.00	0.03	-0.03	-0.03	0.00
1.65	0.01	-0.00	-0.01	-0.00	0.03	-0.02	-0.03	0.00
1.70	0.01	-0.00	-0.01	-0.01	0.02	-0.02	-0.02	0.00
1.75	0.00	-0.01	-0.01	-0.01	0.02	-0.02	-0.02	0.00
1.80	0.00	-0.01	-0.00	-0.01	0.02	-0.01	-0.02	0.00
1.85	0.00	-0.01	-0.00	-0.01	0.02	-0.01	-0.01	0.00
1.90	0.00	-0.01	-0.00	-0.01	0.01	-0.01	-0.01	0.00
1.95	0.00	-0.01	-0.00	-0.01	0.01	-0.01	-0.01	0.00
2.00	0.00	-0.01	-0.00	-0.01	0.01	-0.01	-0.01	0.00

Table 3 (continued).

8 to 9 km and heating decreases rapidly with height above the maxima. The profiles are similar in form to the diurnal and semidiurnal ones (Groves, 1980b) but are on a much smaller scale. Maximum heating rates in mw/kg are shown in Table 4 and contrast with the (2,2,2) October peak of 6.7 mW/kg. As a further comparison, the ozone (3,3,3) October peak is about 60 times greater than its water vapour counterpart, but the two resulting surface pressure oscillations (§ 5) are in the ratio of only 2 to 1.

Table 4. Maximum water vapour heating rates, mW/kg. Negative signs indicate a reversal of phase.

	(3,3,3)	(3,3,4)	(3,3,5)	(3,3,6)
January	0.78	-1.09	-0.14	0.38
April	0.70	0.61	-0.05	-0.28
July	0.74	1.10	-0.21	-0.35
October	0.63	-0.45	-0.03	0.22

5. Surface pressure oscillations

Surface pressure oscillations P_o have been calculated for ozone and water vapour heating profiles by classical tidal theory, the method of analysis being that previously employed for diurnal and semidiurnal components (Groves, 1981). For the (m,m,n) mode, P_o is expressed as

$$P_o = (P_n^{mR} \cos\sigma t' + P_n^{mI} \sin\sigma t') \Theta_n^m \qquad (5.1)$$

where t' is local time and σ is the angular frequency of oscillation. Results are presented in Fig. 8 as plots of P_n^{mI} against P_n^{mR} and are numbered 1,2,3 and 4 for January, April, July and October respectively. The local time $\sigma^{-1} \tan^{-1}(P_n^{mI}/P_n^{mR})$ is shown on each axis in Fig. 8. Amplitudes and phases are given in Tables 5 and 6.

Comparisons are made with the observed values quoted in Butler & Small (1963) which are indicated on Fig. 8 by A for the annual mean and J for a solstitial value. Comparisons are also made with the earlier theoretical results of Siebert (1961) for water vapour heating and Butler & Small (1963) for ozone heating, the combined effects being denoted by S in Fig. 8.

For the (3,3,3) mode, the amplitudes of the results

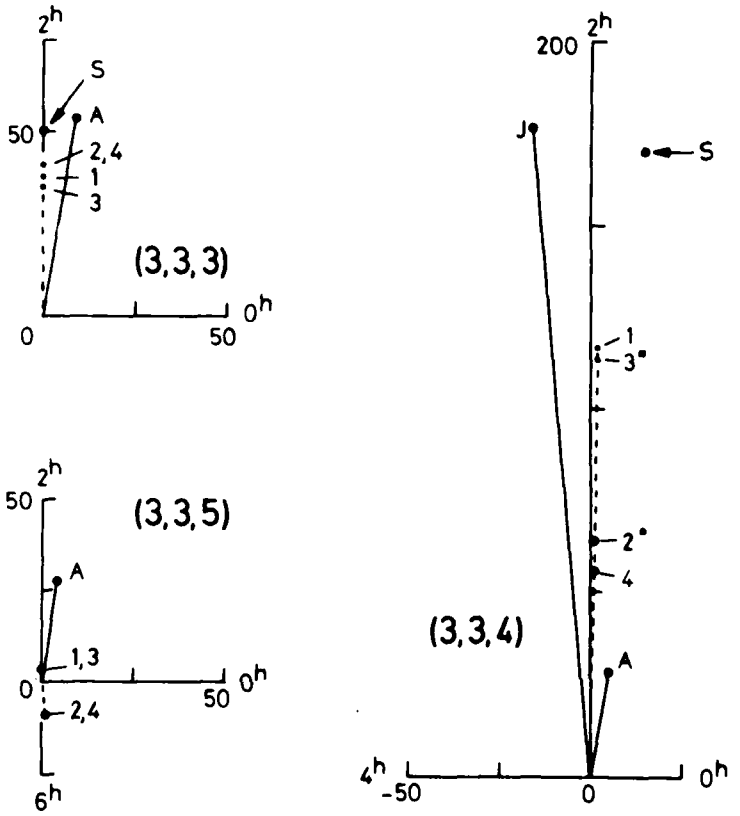

Fig. 8 P_n^{mR} and P_n^{mI} are plotted in μb on the horizontal and vertical axes respectively for modes (3,3,n), n=3,4,5. Local times of maximum ($\omega_n^m > 0$) are shown on each axis. 1,2,3,4 denote calculated values for January, April, July, October. * denotes a value plotted with the sign reversed. S denotes the combined calculations of Siebert (1961) and Butler and Small (1963). A is the observed annual mean and J the observed January or (-) July values quoted by Butler and Small (1963).

Season	1		3		2		4	
	P	Ph	P	Ph	P	Ph	P	Ph
(3,3,3)								
A	-	-	-	-	55	1.78	(annual mean)	
B	38	2.00	35	2.00	42	2.00	41	2.00
C	-	-	48	2.00	50	2.00	(annual mean)	
(3,3,4)								
A	179	1.89	179	-1.89	29	1.78	(annual mean)	
B	117	1.98	113	-2.02	64	-2.02	55	1.98
C	174	2.11	174	-2.11	5	-2.13	(equinox)	
(3,3,5)								
A	-	-	-	-	28	1.78	(annual mean)	
B	2	1.9	3	2.0	8	-1.8	8	-1.8

Table 5. Terdiurnal Hough modes of surface pressure. Values are of $P = \left| P_n^{3R} + iP_n^{3I} \right|$ in μb where P_n^{3R}, P_n^{3I} are defined by (5.1) and of Ph, the local time of maximum ($\Theta_n^3 > 0$) in hours, for modes (3,3,n), n=3,4,5. A are the observational results quoted by Butler & Small (1963); B are the present calculations from Table 6 (total); C are the combined calculated values of Siebert (1961) and Butler & Small (1963). Columns 1,2,3,4 refer to the four seasons. In A, 1 and 3 are for January and July and in C are for the winter and summer solstices. In the present calculations,B, 1,2,3,4 refer to January, April, July and October.

	Water vapour				Ozone				Total			
	P^R	P^I	P	Ph	P^R	P^I	P	Ph	P^R	P^I	P	Ph
(3,3,3)												
Jan	0	15	15	2.00	0	23	23	2.00	0	38	38	2.00
Apr	0	15	15	2.00	0	27	27	2.00	0	42	42	2.00
Jul	0	13	14	2.00	0	22	22	2.00	0	35	35	2.00
Oct	0	14	14	2.00	0	27	27	2.00	0	41	41	2.00
Ann	0	37	37	2.00	0	13	13	1.98	0	50	50	2.00
(3,3,4)												
Jan	0	26	26	2.01	2	91	91	1.97	2	117	117	1.98
Apr	0	-14	14	-1.99	-1	-50	50	-2.03	-1	-64	64	-2.02
Jul	0	-27	27	-1.99	-2	-86	86	-2.03	-2	-113	113	-2.02
Oct	0	11	11	2.01	1	44	44	1.97	1	55	55	1.98
Equ	0	0	0	-	-1	-5	5	-2.13	-1	-5	5	-2.13
Sol	0	45	45	2.00	15	128	129	2.15	15	173	174	2.11
(3,3,5)												
Jan	0	1	1	2.0	0	2	2	1.9	0	2	2	1.9
Apr	0	0	0	-	1	-8	8	-1.8	1	-8	8	-1.8
Jul	0	1	1	2.0	0	2	2	1.9	0	3	3	2.0
Oct	0	1	1	2.0	1	-9	9	-1.8	1	-8	8	-1.8

Table 6. Terdiurnal Hough modes of surface pressure evaluated for water vapour heating and ozone heating. P^R, P^I are the quantities P_n^{3R}, P_n^{3I} defined by (5.1) and are in μb. P and Ph are defined in Table 5. The columns under Total are the sum of the water vapour and ozone contributions. The entries under Jan, Apr, Jul, Oct are the present calculations. Those under Ann (annual mean), Equ (equinox), Sol (solstice, January) are from Siebert(1961) for water vapour and Butler & Small (1963) for ozone.

(1,2,3 and 4 in Fig. 8) are about 20 per cent less than those previously calculated (S), but are still close to the observed value (A), being within about 15 μb. The relative contributions of the two heat sources in the present calculations are however substantially different from the earlier ones, and now amount to 65 per cent from ozone instead of 25 per cent.

The antisymmetric (3,3,4) mode attains its largest values at the solstices. Earlier calculation of solstitial values, denoted by S in Fig. 8, has shown about three-quarters of the amplitude to be generated by ozone heating and that together the two heat sources account adequately for the observed value (J). In the present calculation ozone heating again accounts for about three-quarters of the total amplitude, but this amount, denoted by 1 or 3* in Fig. 8, is now only 64 per cent of that observed.

Fig. 8 includes a plot of (3,3,5) values although amplitudes are probably too small for any useful comparison to be made between theory and observation.

6. Discussion

Previous work on the diurnal and semidiurnal components of ozone and water vapour heating and their contributions to surface pressure has been extended to the terdiurnal component. Although much smaller than the diurnal and semidiurnal components, the terdiurnal is dominated at the solstices by its (3,3,4) mode with an amplitude of 179 μb and comparisons between theory and observation can reasonably be made. Previous calculations by Siebert (1961) for terdiurnal water vapour heating and Butler & Small (1963) for terdiurnal ozone heating have given a total surface pressure oscillation in very close agreement with observation, not only for the (3,3,4) mode but also for the smaller (3,3,3) mode of amplitude 55 μb (Fig. 8).

The present results for the (3,3,4) mode agree closely with the previous ones in phase but differ in amplitude accounting for only 64 per cent of the observational value (Fig. 8). Although ozone generates much (about ¾) of the surface pressure oscillation, the decrease is not readily attributed to changes in the ozone heating profile as the present (3,3,4) solstitial profile and the earlier values of Butler & Small (1963) are in good agreement (Fig. 3). Attention has therefore been given to the effect of the

basic temperature profile on the calculated surface pressure. Butler & Small (1963) adopted a temperature profile from Murgatroyd (1957) up to 100 km and extended it to 150 km with a thermospheric gradient of 4 K/km. The 50 km maximum had a value of about 295 K and the 80 km minimum 203 K. Compared with the profile used in the present work, the 50 km temperature was higher by 23 K, the mesopause temperature was higher by 8 K and lower in altitude by about 10 km and the thermospheric gradient rose at a lower rate. The present scale heights at 0(2)26 km are 8.75, 8.46, 8.14, 7.82, 7.53, 6.98, 6.63, 6.22, 5.90, 5.99, 6.14, 6.24, 6.39, 6.56 km and at 28(2)150 km are taken from the mean CIRA (1972). When the (3,3,4) mode is re-calculated with the present heating and the basic temperature profile used by Butler & Small (1963), the ozone contribution to the surface pressure is increased by about 58 per cent and a total amplitude is obtained for July of 155 μb instead of the present 113 μb. The change to a more realistic basic temperature profile is therefore the main factor leading to the present reduced values.

We need to note that the present calculations have been based on classical tidal theory which ignores mean winds and latitudinal temperature gradients. Walterscheid et al.

(1980) evaluated semidiurnal modes under both classical and non-classical assumptions and found that the introduction of mean winds and temperature gradients increased the solstitial values of the (2,2,2) surface pressure by 18 per cent. The vertical structure of the (3,3,4) mode is very similar to that of the (2,2,2) as their equivalent depths are nearly equal, being 7.66 and 7.85 km respectively, and the (3,3,4) surface pressure amplitude is likely to be modified by a similar order of magnitude. Without detailed calculations, we can only note that the 64 μb discrepancy between observation and classical theory will be affected by non-classical effects, possibly by as much as 20 μb.

7. Conclusions

The very close agreement reported (Butler & Small, 1963) between the observed and calculated amplitudes of the (3,3,4) mode is found to be fortuitous as it depends on the choice of a basic temperature profile which is no longer acceptable. The present calculations underpredict the observed solstitial (3,3,4) amplitude by about 64 μb, i.e. 36 per cent. The significance of this difference is uncertain as observational accuracy has not been defined, but previous

evaluation of diurnal and semidiurnal components (Groves, 1981) has underpredicted observed values and it is therefore not unreasonable for the terdiurnal component to be underpredicted by the same analytical procedure.

Acknowledgements - Sponsorship has been provided for this work by the Air Force Geophysics Laboratory (AFGL), United States Air Force under Grant No. AFOSR - 77 - 3224. The assistance of Mr. Jonathan D. Groves with data preparation and computer processing on the GEC 4082 machines (EUCLID) at University College London is very gratefully acknowledged.

REFERENCES

BUTLER, S.T. & SMALL, K.A. (1963) Proc. R. Soc. Lond. A274, 91-121.

GROVES, G.V. (1979) Notes on obtaining the eigenvalues of Laplace's tidal equation, in Interim Scientific Report No. 3, AFOSR-77-3224, Department of Physics and Astronomy, University College London, Gower Street, London WC1E 6BT, England, 31 December 1979.

GROVES, G.V. (1980a) Hough components of ozone heating, in Interim Scientific Report No. 4, AFOSR-77-3224, Department of Physics and Astronomy, University College London, Gower Street, London WC1E 6BT, England, 30 June 1980.

GROVES, G.V. (1980b) Hough components of water vapour heating, in Final Scientific Report, Part I, AFOSR-77-3224, Department of Physics and Astronomy, University College London, Gower Street, London WC1 6BT, England, 31 December 1980.

GROVES, G.V. (1981) Diurnal and semi-diurnal Hough components of surface pressure, in this Report.

HANN, J. v. (1918) Denkschr. Akad. Wiss. Wien Math.-nat. Kl. 95, 1-64.

LUCAS, R.J. (1978) A latitudinal and seasonal ozone model to 75 km, in Scientific Report AFOSR-77-3224 by Groves, G.V. and Lucas, R.J., Department of Physics and Astronomy, University College London, Gower Street, London WC1E 6BT, England, 31 December 1978.

MURGATROYD, R.J. (1957) Quart. J. R. Met. Soc., 83, 417-

NEWELL, R.E., KIDSON, J.W., VINCENT, D.G. & BOER, G.J. (1972) The General Circulation of the Tropical Atmosphere and Interactions with Extratropical Latitudes, Volume I, The M.I.T. Press.

SIEBERT, M. (1961) Adv. Geophys. 7, 105-182.

WALTERSCHEID, R.L., DeVORE, J.G. & VENKATESWARAN, S.V. (1980) J. Atmos. Sci. 37, 455-470.

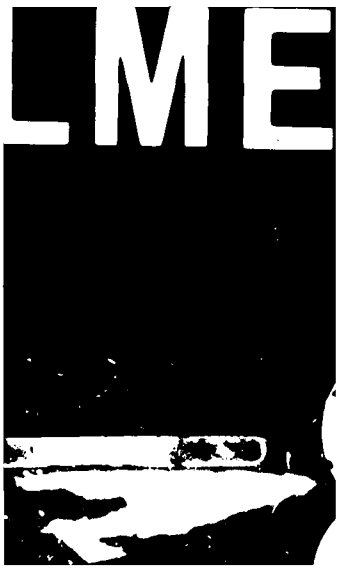
LME